CANDY

Comorbid Analysis of Neurodevelopmental Disorders and epilepsY

Deliverable D1.3

Report on effects of neuroinflammation during early development

Grant Agreement number: 847818 SC1-BHC-01-2019

Start date of project: 1 January 2020 Duration: 66 months

Lead beneficiary: UULM

Due date of deliverable: 31/12/2024 Actual submission date: 20/12/2024

Document type: Report

Dissemination Level

PU Public

This project has received funding from the European Union's Horizon 2020 Research and Innovation Programme under grant agreement No. 847818.

Table of Contents

1 Executive summary

Autism Spectrum Disorders (ASD) are mainly characterized by deficits in social interaction and communication and by repetitive and rigid behaviours. Known causes of ASD are mutations of certain risk genes like the postsynaptic protein SHANK3 and environmental factors including prenatal infections. To analyse the gene-environment interplay in ASD we combined the *Shank3ΔE11-/-* ASD mouse model with Maternal Immune Activation (MIA) via an intraperitoneal injection of polyinosinic:polycytidylic acid (Poly I:C) on gestational day 12.5. The offspring of the injected dams was further analysed for autistic-like behaviours (*Bauer et al., 2022*) and comorbidities followed by biochemical experiments with a focus on synaptic protein expression. We show that the two-hit mice exhibit excessive grooming and deficits in social behaviour more prominently than the *Shank3ΔE11-/-* mice. Interestingly these behavioural changes were accompanied by an unexpected upregulation of postsynaptic density (PSD) proteins at excitatory synapses in striatum, hippocampus and prefrontal cortex. We could demonstrate that there is an interplay between genetic susceptibility and environmental factors defining the severity of ASD symptoms. Moreover, we show that a general misbalance of PSD proteins at excitatory synapses are linked to ASD symptoms, making this two-hit model a promising tool for the investigation of the complex pathophysiology of neuropsychiatric disorders.

(The study has been published as: Atanasova et al., 2023; accordingly, parts of the text and figures are taken from Atanasova et al., 2023)).

2 Introduction

Autism Spectrum Disorders (ASD) are complex neurodevelopmental disorders characterized by two main symptoms – (i) deficits in social interaction and communication and (ii) restricted and repetitive behaviours [1]. The term "spectrum" has been introduced to indicate the heterogeneity of symptoms seen in autistic people as well as the variety of causes. In addition, several comorbidities are associated with ASD including intellectual disability, language impairment and motor deficits amongst others. Regarding the causes of ASD, twin and family studies suggest a strong genetic contribution. Interestingly, among the autism risk genes are several genes coding for synaptic proteins like the SHANK family of postsynaptic scaffolding molecule. SHANKs are highly concentrated at postsynaptic densities of excitatory synapses and play a key role in synaptogenesis and synaptic plasticity, especially during postnatal brain development. Thorough analyses of stratified patient cohorts revealed that there is a gradient of severity when it comes to the different members of this protein family, with SHANK3 mutations being the most common (0.69% of ASD patients) and leading to the most severe phenotype. Moreover, in most cases, the heterogeneous disruption or deletion of SHANK3 has been shown to lead to a syndromic form of autism, the Phelan-McDermid Syndrome. Over the years, several mouse models carrying mutations in the Shank3 gene have been generated. These knockout mice presented reduced interest for social interaction in the three-chambers test and free social interaction including abnormalities in the emission of ultrasonic vocalizations (USVs). The models also displayed repetitive self-grooming as well as specific synaptic abnormalities such as a reduction in the number of synapses. While there is a significant genetic component in ASD, many studies indicate that certain environmental factors significantly contribute to the pathogenesis of ASD. A higher risk to develop ASD for dizygotic twins compared to non-twin siblings hints at a role for the maternal environment. Epidemiological studies have associated the occurrence of a viral infection during the first and second trimester of pregnancy with an increased risk for the children to develop ASD, while a weaker link was found for a bacterial infection. Thus, Maternal Immune Activation

(MIA) mouse models have been created in order to study the mechanisms through which an early life infection might cause long-term behavioural defects. Polyinosinic:polycytidylic acid (Poly I:C) is commonly used to mimic immune activation by a viral infection. This synthetic dsRNA molecule interacts with toll-like receptor-3 (TLR-3) and increases the production of proinflammatory cytokines and chemokines in the embryonic brain. Behavioural abnormalities related to ASD like decreased social recognition and communication have been found in the offspring of mice following an immune activation with Poly I:C, as well as increased repetitive behaviours. Moreover, these mouse models present reduced dendritic branching and dendritic spine density and altered synaptic transmission in the hippocampus.

Two-hit preclinical models are based on the hypothesis that multiple factors, genetic and environmental, converge and lead to the development of the adult pathology. Two-hit and even multiple-hit rodent models have been extensively used in schizophrenia research. Concerning autism, some studies have combined two environmental factors and have found a worsening of the autistic-like phenotype. However, only a few autism-related studies have combined environmental factors with genetic susceptibility. Interestingly, the application of valproic acid (VPA) and propionic acid (PPA) was found to induce alterations in the expression of SHANK proteins in those models.

To further elucidate the interplay of internal (genetic disposition) and external factors (environment) related to Shank3 ASD we combined a partial knockout mouse model Shank3Δ11-/- with MIA by intraperitoneal injection of Poly I:C on gestational day (GD) 12.5. In this two-hit model the core symptoms of autism as well as comorbidities are investigated by the means of a wide set of behavioural experiments.

3 Main section

3.1 Two Hit Mouse Model

Wild type and *Shank3* heterozygous pregnant mice received an intraperitoneal injection of the synthetic virus Poly I:C or saline on GD12.5 (Figure 1A). Heterozygous breedings lead to the creation of six experimental groups – wild type (WT), *Shank3* heterozygous (Het) and knockout (KO) offspring of a saline-injected and poly I:C-injected *Shank3* Het dams, respectively (Figure 1B). To control for a possible impact of the genotype of the dams, wild type dams were injected as well (Figure 1B). The occurrence of a systemic inflammation in those mice was confirmed by an ELISA analysis for Interleukin 6 (IL-6). Three hours post-injection, there was a significant increase in the IL-6 concentration in the blood serum of both WT and *Shank3* Het mice (Figure 1C). The genotype of the mother had no effect indicating that both dams reacted similarly to the injection of the synthetic virus. The inflammation was transitory, for nine hours post-injection no significant differences in IL-6 concentration were found (Figure S1A). Moreover, the treatment with Poly I:C led to a significant decrease in body temperature three to nine hours post-injection. The temperature was back to normal 24 hours after the injection of Poly I:C, however, the dams that suffered an abortion had a significant weight loss (Figure 1D). This weight loss was indicative of the abortion as in the Poly I:C group 55-60% of the mice lost the embryos (Figure 1E). The Poly I:C treatment did not lead to premature birth but showed an increase in the pre-weaning mortality. Both groups (saline and Poly I:C) gave birth to a similar number of pups presenting expected sex and genotype ratios implying that two-hit mice were not less likely to survive. Finally, the weight gain from conception until the day before the injection was comparable between all groups meaning that the higher abortion rate in the poly I:C-injected dams was not due to them carrying more. The Poly I:C injection caused a severe reaction in the dams manifesting with a transitory systemic inflammation and body temperature decrease that was leading to higher abortion rates and increased pre-weaning mortality of the pups.

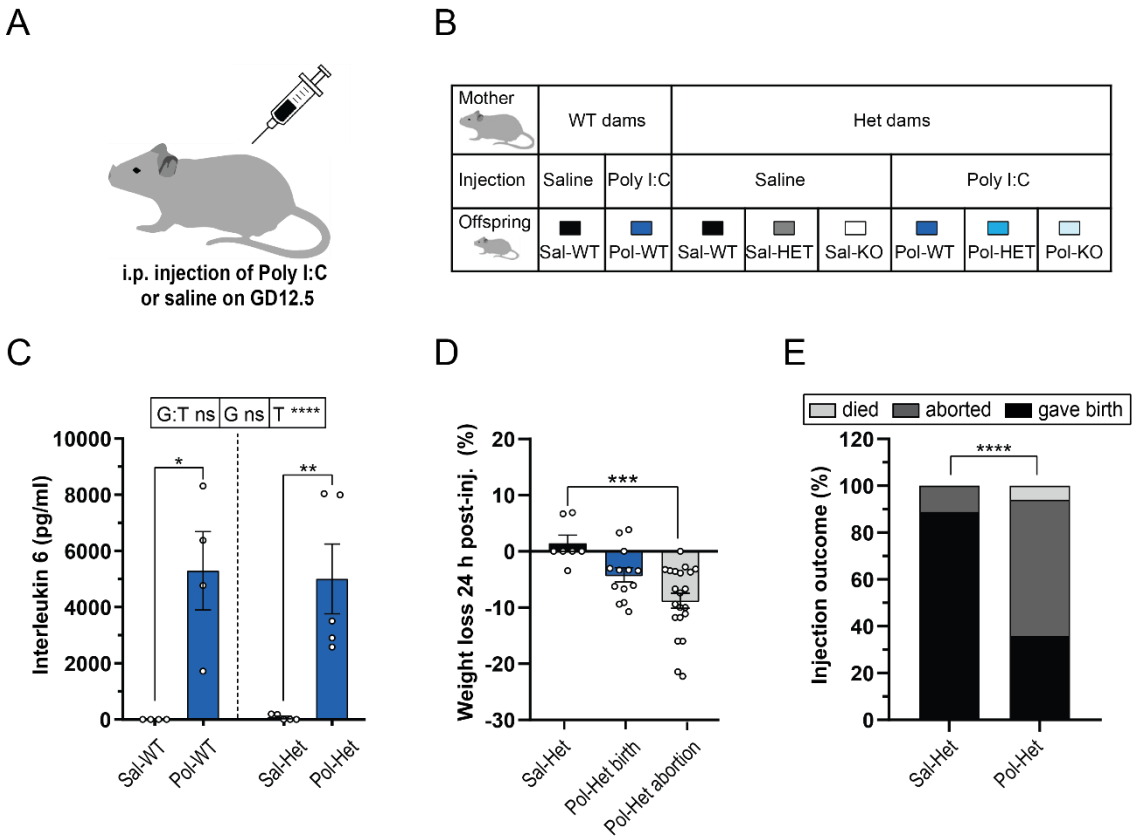

Figure 1. Experimental design and dam response to the injection of the synthetic virus A An intraperitoneal (i.p.) injection of saline or Poly I:C was performed in pregnant mice on gestational day (GD) 12.5**. B** Table describing all the experimental groups. **C** Interleukin 6 blood serum concentration (pg/ml) three hours post-injection. T ****p<0.0001, Sal-WT vs Pol-WT *p=0.0114 and Sal-Het vs Pol-Het **p=0.0085. Data were analyzed by two-way ANOVA followed by a Bonferroni correction for multiple comparisons. Sal-WT n=4, Pol-WT n=4, Sal-Het n=5, Pol-Het n=5. G = Genotype of the mother; T = Treatment of the mother; G:T = interaction between the two factors. **D** Weight lost (%) 24 hours post-injection. Sal-Het vs Pol-Het abortion ***p=0.0005. Data were analyzed by Kruskal-Wallis followed by Dunn's correction for multiple comparisons. Sal-Het n=7, Pol-Het birth n=13, Pol-Het abortion n=21. **E** Injection outcome (%). Sal-Het vs Pol-Het ****p<0.0005. Data were analyzed by Pearson Chi-square test (expected frequencies ≥ 5), two-sided. Sal-Het birth n=16, Sal-Het abortion n=2, Pol-Het birth n=24, Pol-Het abortion n=39, Pol-Het death n=4. **C-E** Data were tested for normality with the Shapiro-Wilk test. Significance level was set to 0.05 (#<0.10, *p<0.05, **p<0.01, ***p<0.001, ****p<0.0001). Mean ± SEM. ns = not significant.

3.2 Core symptoms of autism

Next, the core symptoms of ASD were assessed in the adult offspring of the injected dams. First, alterations in social behaviour and communication were investigated. During the same-sex reciprocal social interaction test, male mice spent the same amount of time in contact (Figure 2A) and made the same number of contacts (Figure S2A). Mice that displayed excessive aggression were excluded from the analysis as the goal of the test was to assess exclusively affiliative social interaction. Moreover, the two-hit mice were not the ones to

initiate the first contact (Figure 2B). This social approach deficit was confirmed during phase two of the three chambers test where the two-hit mice were the only group that did not show a preference in spending time with their conspecific (Figure 2C). During the last phase of the test, Pol-WT, Sal-KO and two-hit mice showed a social recognition alteration (Figure 2D). Furthermore, during the habituation phase of the three chambers test all groups showed no innate preference towards one of the rooms. Addressing the second core symptom of ASD - repetitive behaviour - the two-hit mice spent a significantly longer time self-grooming compared to the Pol-WT and Sal-KO groups (Figure 2E). In addition, each grooming event of the mice in the two KO groups lasted longer resulting in an increase in the grooming bout duration. Contrary to the Sal-KO group, the Pol-KO mice did not spend more time self-grooming (Figure 2E). However, these mice displayed a significant increase in the time spent digging while the KO groups showed a decrease of this behaviour (Figure 2F).

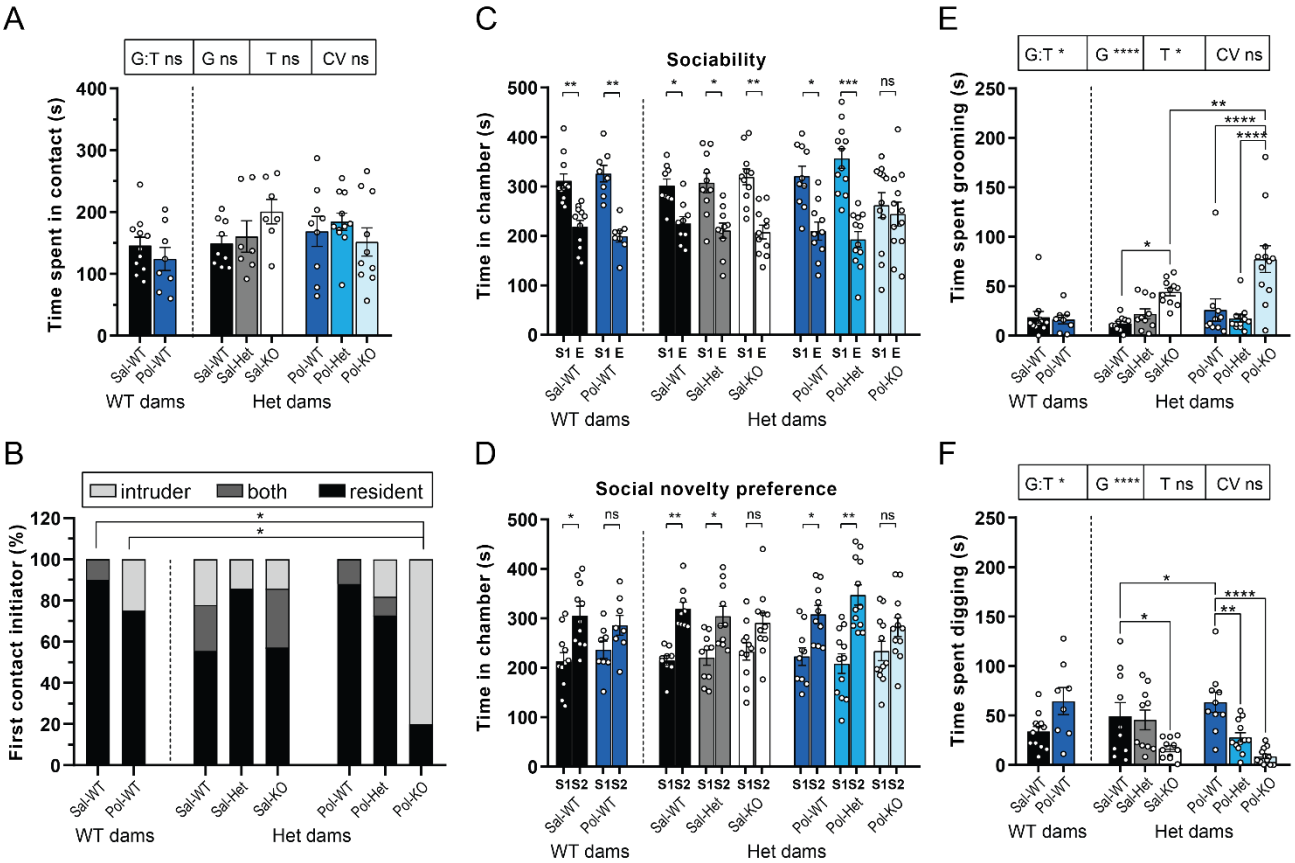

Figure 2. Core symptoms of autism A Time spent in contact (s) during same-sex reciprocal social interaction. Data were analyzed by two-way ANCOVA followed by a Bonferroni correction for multiple comparisons. G = Genotype of the offspring; T = Treatment of the mother; G:T = interaction between the two factors; CV = covariate "Genotype of the mother". **B** Initiator of the first contact (%) during same-sex reciprocal social interaction. Pol-KO vs the following: Sal-WT (WT dams) **p=0.0052 and Pol-WT (WT dams) **p=0.0018. Data were analyzed by pairwise Fisher's exact test followed by a Benjamin-Hochberg correction for multiple comparisons. **C** Time spent in chamber

(s) during the sociability phase of the three chambers test. Sal-WT (WT dams) **p=0.0061, Pol-WT (WT dams) **p=0.0025, Sal-WT (Het dams) *p=0.0199, Sal-Het *p=0.0215, Sal-KO **p=0.0037, Pol-WT (Het dams) *p=0.0138, Pol-Het ***p=0.0007. **D** Time spent in chamber (s) during the social novelty preference phase of the three chambers test. Sal-WT (WT dams) *p=0.0285, Sal-WT (Het dams) **p=0.0019, Sal-Het *p=0.0327, Pol-WT (Het dams) *p=0.0389, Pol-Het **p=0.0048. **E** Time spent self-grooming (s). G:T *p=0.0310, G ****p<0.0005 and T *p=0.0450, Sal-KO vs Sal-WT *p=0.0210 and Pol-KO vs the following: Sal-KO **p=0.0020, Pol-WT ****p<0.0005 and Pol-Het ****p<0.0005. **F** Time spent digging (s). G:T *p=0.0110 and G ****p<0.0005, Sal-WT vs the following: Pol-WT *p=0.0100 and Sal-KO *p=0.0260. Pol-WT vs the following: Pol-Het **p=0.0010 and Pol-KO ****p<0.0005. **A-B** Sal-WT (WT dams) n=11, Pol-WT (WT dams) n=8, Sal-WT (Het dams) n=9, Sal-Het n=7, Sal-KO n=7, Pol-WT (Het dams) n=9, Pol-Het n=11, Pol-KO n=10. **C-D** Data were analyzed by a paired two-tailed t-test (when normal) or by Wilcoxon matched-pairs signed rank two-tailed test (when not normal). Sal-WT (WT dams) n=11, Pol-WT (WT dams) n=8, Sal-WT (Het dams) n=9, Sal-Het n=10, Sal-KO n=11, Pol-WT (Het dams) n=10, Pol-Het n=12, Pol-KO n=12. E = Empty cage, S1 = Stranger 1, S2 = Stranger 2. **E-F** Data were analyzed by two-way ANCOVA followed by a Bonferroni correction for multiple comparisons. Sal-WT (WT dams) n=12, Pol-WT (WT dams) n=8, Sal-WT (Het dams) n=10, Sal-Het n=10, Sal-KO n=11, Pol-WT (Het dams) n=10, Pol-Het n=12, Pol-KO n=12. G = Genotype of the offspring; T = Treatment of the mother; G:T = interaction between the two factors; CV = covariate "Genotype of the mother". **A-F** Data were tested for normality with the Shapiro-Wilk test. Significance level was set to 0.05 (#<0.10, *p<0.05, **p<0.01, ***p<0.001, ****p<0.0001). Mean ± SEM. ns = not significant.

In addition, the Sal-KO mice emitted a significantly higher amount of ultrasonic vocalizations (Figure 3A). Two-hit mice presented a decrease in the number of calls compared to Sal-KO (Figure 3A). Moreover, Sal-KO male mice were the only group that did not contain any "low" vocalizers. Therefore, in the qualitative analysis of the different call types emitted by the mice, only the "average" and "high" vocalizers were included while all mice that emitted less than 5.25 calls in total were excluded (Figure S3B). After classifying the calls, chevron, step down, down fm (frequency modulation) and step up calls seemed to be altered in Sal-KO and Pol-KO (Figure 3B). Both KO groups emitted more chevron (Figure 3C) and step down calls (Figure 3D) yet only Sal-KO mice presented with a higher amount of down fm calls (Figure 3E), all three being USV types ending at a lower frequency. Moreover, Pol-WT mice emitted less step down (Figure 3D) and step up calls (Figure 3F), indicating that the Poly I:C treatment caused a decrease in the number of calls with frequency jumps in the WT offspring. Finally, both KO mice emitted more step up calls (Figure 3F). No further differences in USV types were found between the groups except of a decrease in the percentage of short calls emitted by Sal-KO mice compared to Sal-Het.

3.3 Autism-related comorbidities

Both KO groups showed a similar decrease in locomotion (Figure 3G). Those mice spent the same amount of time in the center of the open field arena as the other groups (Figure S5A)

but they made fewer entries into the center (Figure 3H). Moreover, Sal-KO and Pol-KO male mice showed an avoidance behaviour during the marble burying test where they would not bury the objects (Figure 3I).

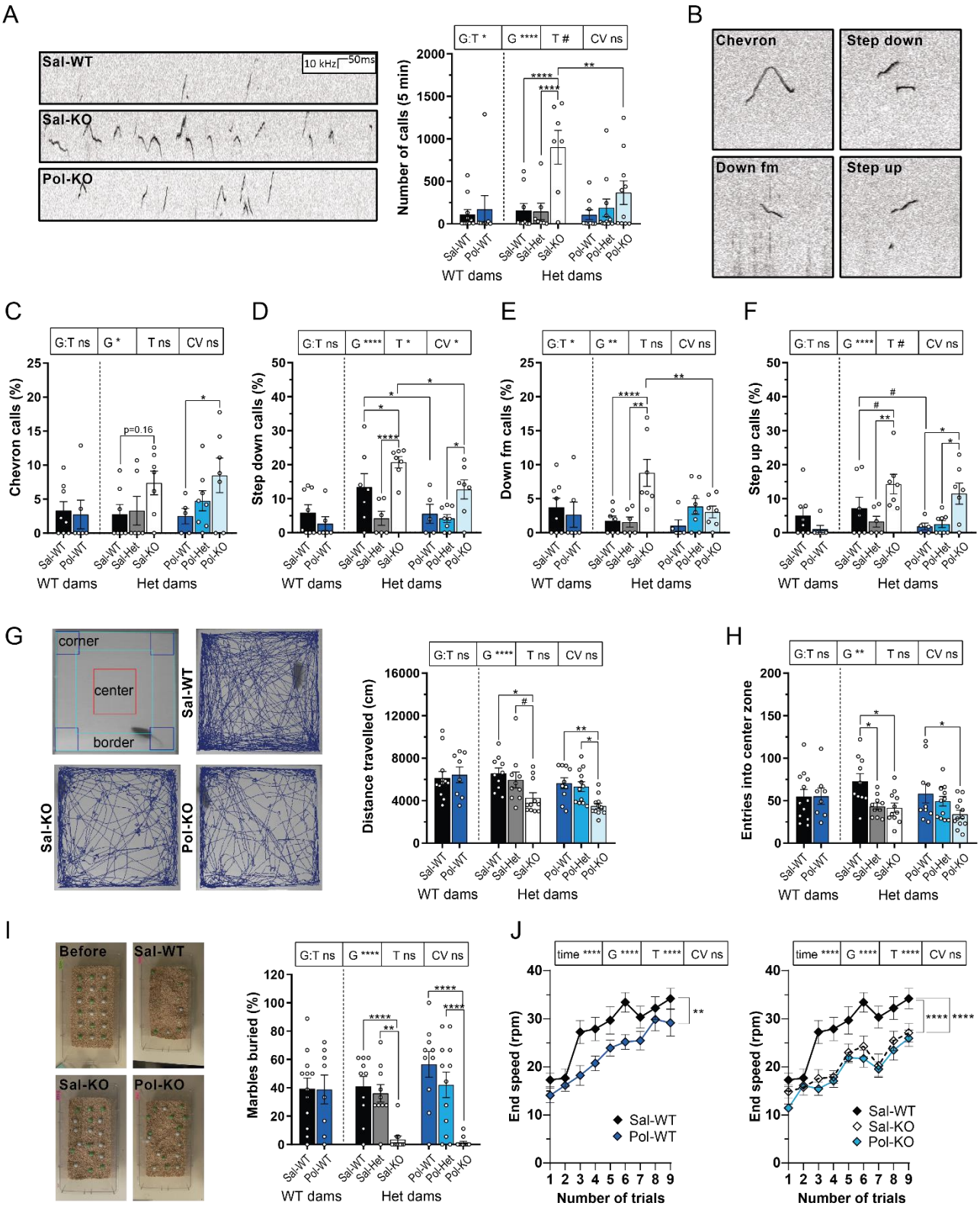

Figure 3. Deficits in ultrasonic vocalizations and comorbidities A Spectrogram of calls emitted by Sal-WT, Sal-KO and Pol-KO mice. Total number of calls emitted over 5 min during same-sex reciprocal social interaction. G:T *p=0.0190, G ****p<0.0005, T #p=0.0660, Sal-

KO vs the following: Sal-WT ****p<0.0005, Sal-Het ****p<0.0005 and Pol-KO **p=0.002. Sal-WT (WT dams) n=11, Pol-WT (WT dams) n=8, Sal-WT (Het dams) n=9, Sal-Het n=7, Sal-KO n=7, Pol-WT (Het dams) n=9, Pol-Het n=11, Pol-KO n=10. **B** Spectrograms of chevron, step down, down fm and step up call types. fm = frequency modulation. **C** Percentage of chevron calls. G *p=0.0130. Sal-WT vs Sal-KO p=0.1660 and Pol-WT vs Pol-KO *p=0.0480. **D** Percentage of step down calls. G ****p<0.0005, T *p=0.0190, CV *p=0.0330, Sal-KO vs the following: Sal-WT *p=0.0390, Sal-Het ****p<0.0005 and Pol-KO *p=0.0240. Sal-WT vs Pol-WT *p=0.0400. Pol-Het vs Pol-KO *p=0.0400. **E** Percentage of down fm calls. G:T *p=0.0100, G **p=0.0030, Sal-KO vs the following: Sal-WT ****p<0.0005, Sal-Het **p=0.0010 and Pol-KO **p=0.0020. **F** Percentage of step up calls. G ****p<0.0005, T p=0.1190, Sal-KO vs the following: Sal-WT #p=0.0510 and Sal-Het **p=0.0050. Pol-KO vs the following: Pol-WT *p=0.0160 and Pol-Het *p=0.0170. Sal-WT vs Pol-WT #p=0.0590. **G** Representative figures of the zones in the open field arena and the distance travelled by Sal-WT, Sal-KO and Pol-KO. Total distance travelled (cm) in the open field arena. G ****p<0.0005, Sal-KO vs the following: Sal-WT *p=0.0200 and Sal-Het #p=0.0950. Pol-KO vs the following: Pol-WT **p=0.0020 and Pol-Het *p=0.0400. **H** Number of entries into the center zone of the open field. G **p=0.0010, Sal-WT vs the following: Sal-Het *p=0.0350 and Sal-KO *p=0.0190. Pol-WT vs Pol-KO *p=0.0140. **I** Representative pictures of the marble burying test – before and after for Sal-WT, Sal-KO and Pol-KO. Percentage of marbles buried. G ****p<0.0005, Sal-KO vs the following: Sal-Het **p=0.0050 and Sal-WT ****p<0.0005. Pol-KO vs the following: Pol-Het ****p<0.0005 and Pol-WT ****p<0.0005. **J** End speed (rpm) during the Rotarod test. G:T ns, time ****p<0.0001, G ****p<0.0001 and T ****p<0.0001, Sal-WT vs Pol-WT **p=0.0049. Sal-WT vs the following: Sal-KO ****p<0.0001 and Pol-KO ****p<0.0001. Sal-WT (WT dams) n=12, Pol-WT (WT dams) n=8, Sal-WT (Het dams) n=10, Sal-Het n=8, Sal-KO n=11, Pol-WT (Het dams) n=10, Pol-Het n=6, Pol-KO n=12. **C-F** Sal-WT (WT dams) n=11, Pol-WT (WT dams) n=8, Sal-WT (Het dams) n=9, Sal-Het n=7, Sal-KO n=7, Pol-WT (Het dams) n=9, Pol-Het n=11, Pol-KO n=10. **G-I** Sal-WT (WT dams) n=12, Pol-WT (WT dams) n=8, Sal-WT (Het dams) n=10, Sal-Het n=10, Sal-KO n=11, Pol-WT (Het dams) n=10, Pol-Het n=12, Pol-KO n=12. **A-J** Data were tested for normality with the Shapiro-Wilk test. Rotarod data were analyzed by a linear mixed model analysis with repeated measures followed by a Tukey-Kramer correction for multiple comparisons and all other data by two-way ANCOVA followed by a Bonferroni correction for multiple comparisons. Significance level was set to 0.05 (#<0.10, *p<0.05, **p<0.01, ***p<0.001, ****p<0.0001). Mean ± SEM. G = Genotype of the offspring; T = Treatment of the mother; G:T = interaction between the two factors; CV = covariate “Genotype of the mother”; ns = not significant.

Finally, the motor abilities of the adult offspring were investigated via the Rotarod test. A motor coordination deficit was present in the WT offspring of poly I:C-treated dams (Figure 3J). An even more severe deficit was found in the Sal-KO and two-hit mice while both KO groups performed in a comparable way during the experiment (Figure 3J). However, all experimental groups were able to improve their motor coordination over time, meaning that they had no motor learning alterations.

3.4 Brain region-specific alterations of postsynaptic proteins in two-hit mice

To comprehend if these behavioural changes co-occur with biochemical alterations, brain tissue lysates of the eight offspring groups have been collected (see Figure 1B). Homogenates and the P3 fraction of striatum, hippocampus and prefrontal cortex (PFC) have been analysed using Western Blotting, to compare protein expression in total protein lysate and the postsynaptic density. The SHANK3 antibody used in this study was validated

in a recent paper. Successful fractionation of the offspring of WT dams was confirmed by Western Blotting for PSD95 (postsynaptic) and SYNAPTOPHYSIN (SYN, presynaptic). Poly I:C injection in WT dams only revealed minor changes in the tissue homogenate of the WT offspring, but no changes in the P3 fractions. In striatum, only the SHANK3c/d isoform was slightly increased in homogenate.

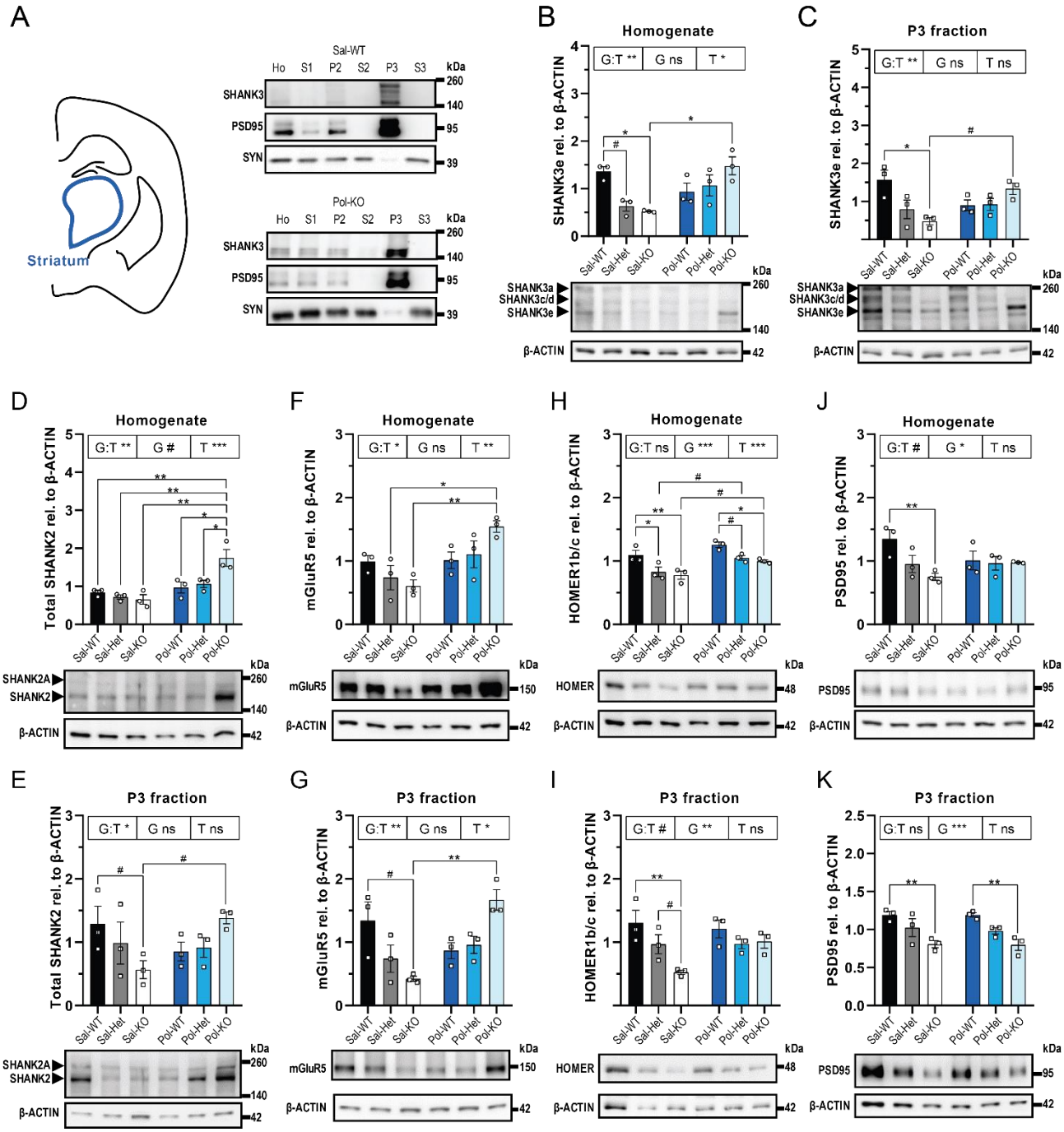

Figure 4. Synaptic changes in striatum of the offspring of Het dams. A Fractionation of the striatum. Western Blots of Sal-WT and Pol-KO are shown for SHANK3, PSD95 (postsynaptic) and SYNAPTOPHYSIN (SYN, presynaptic)**. B** Western Blot analysis for SHANK3 and β-ACTIN of striatum homogenate. The SHANK3e isoform was analyzed. G:T **p=0.0021; T *p=0.0227, Pol-KO vs Sal-KO *p=0.0114, Sal-WT vs Sal-KO *p=0.0301, Sal-WT vs Sal-Het #p=0.0756. **C** Western Blot analysis for SHANK3 and β-ACTIN of striatum P3 fraction. The SHANK3e isoform was analyzed. G:T **p=0.0040, Pol-KO vs Sal-KO #p=0.0842, Sal-KO vs sal-WT *p=0.0155. **D** Western Blot analysis for SHANK2 and

β-ACTIN of striatum homogenate. The total SHANK2 was analyzed. G:T **p=0.0075, G #p=0.0585, T ***p=0.0004, Pol-KO vs the following: Sal-WT **p=0.0052, Sal-Het **p=0.0018, Sal-KO **p=0.0010, Pol-WT *p=0.0173, Pol-Het *p=0.0440. **E** Western Blot analysis for SHANK2 and β-ACTIN of striatum P3 fraction. The total SHANK2 was analyzed. G:T *p=0.0296, Sal-KO vs Pol-KO #p=0.0510, Sal-WT vs Sal-KO #p=0.0909. **F** Western Blot analysis for mGluR5 and β-ACTIN of striatum homogenate. G:T *p=0.0236, T **p=0.0028, Sal-Het vs Pol-KO *p=0.0285, Sal-KO vs Pol-KO **p=0.0091. **G** Western Blot analysis for mGluR5 and β-ACTIN of striatum P3 fraction. G:T **p=0.0017, T *p=0.0450, Sal-KO vs Pol-KO **p=0.0058, Sal-WT vs Sal-KO #p=0.0565. **H** Western Blot analysis for HOMER1b/c and β-ACTIN of striatum homogenate. G ***p=0.0006, T ***p=0.0010, Sal-WT vs Sal-KO **p=0.0055, Pol-WT vs Pol-KO *p=0.0221, Sal-WT vs Sal-Het *p=0.0184, Pol-WT vs Pol-Het #p=0.0702, Pol-Het vs Sal-Het #p=0.0542, Pol-KO vs Sal-KO #p=0.0505. **I** Western Blot analysis for HOMER1b/c and β-ACTIN of striatum P3 fraction. G:T #p=0.0928, G **p=0.0085, Sal-WT vs Sal-KO **p=0.0032, Sal-Het vs Sal-KO #p=0.0954. **J** Western Blot analysis for PSD95 and β-ACTIN of striatum homogenate. G:T #p=0.0761, G *p=0.0447, Sal-WT vs Sal-KO **p=0.0084. **K** Western Blot analysis for PSD95 and β-ACTIN of striatum P3 fraction. G ***p=0.0003, Sal-WT vs Sal-KO **p=0.0042, Pol-WT vs Pol-KO **p=0.0035. **B-K** Data were tested for normality with the Shapiro-Wilk test followed by two-way ANOVA with a Bonferroni correction for multiple comparisons. Significance level was set to 0.05 (#<0.10, *p<0.05, **p<0.01, ***p<0.001, ****p<0.0001). Mean ± SEM, n=3. G = Genotype of the offspring; T = Treatment of the mother; G:T = interaction between the two factors; ns = not significant.

In hippocampus, the SHANK3e isoform was slightly increased, and HOMER1b/c slightly decreased in homogenate (Figure S8A and S8G) and no changes were observed in PFC. However, the offspring of the *Shank3* Het dams were affected by the Poly I:C dependent on their genotype. In striatum, fractionation was conducted successfully (Figure 4A). SHANK3 levels, total as well as individual isoforms, were decreased in the Sal-Het and Sal-KO as expected both in homogenate and the P3 fraction. However, SHANK3e was specifically increased in the Pol-KO, both in homogenate (Figure 4B) and the P3 fraction (Figure 4C). Moreover, also SHANK2 was significantly increased in the Pol-KO both in homogenate (Figure 4D) and the P3 fraction (Figure 4E) and the same was also observed for mGluR5 (Figure 4F and G). HOMER1b/c and PSD95 were both decreased in the Sal-KO compared to Sal-WT but Poly I:C had no effect (Figure 4H and K).

In the hippocampus, the same fractionation was performed (Figure 5A), and the SHANK3 expression was strongly affected by both the genotype and the Poly I:C treatment. In homogenate, the total SHANK3 and all isoforms analyzed were reduced in Sal-KO compared to Sal-WT (Figure 5B). SHANK3 total, SHANK3a and SHANK3c/d were also reduced in Pol-KO compared to Pol-WT (Figure S12A), but SHANK3e was increased in Pol-KO compared to all other groups (Figure 5B). The same changes but with even higher significance were observed in the P3 fraction (Figure S12B and Figure 5C). SHANK2 followed the same dynamics as in the striatum with a decrease in Sal-KO and an increase in Pol-KO (Figure 5D and E), as well as mGluR5 (Figure 5F and G). HOMER1b/c was decreased in Sal-KO (Figure 5H and I), especially in the P3 fraction there was a strong decrease observed that got increased

back to Sal-WT level upon Poly I:C treatment comparable to SHANK3, SHANK2 and mGluR5. PSD95 was not changed in the hippocampus (Figure 5J and K).

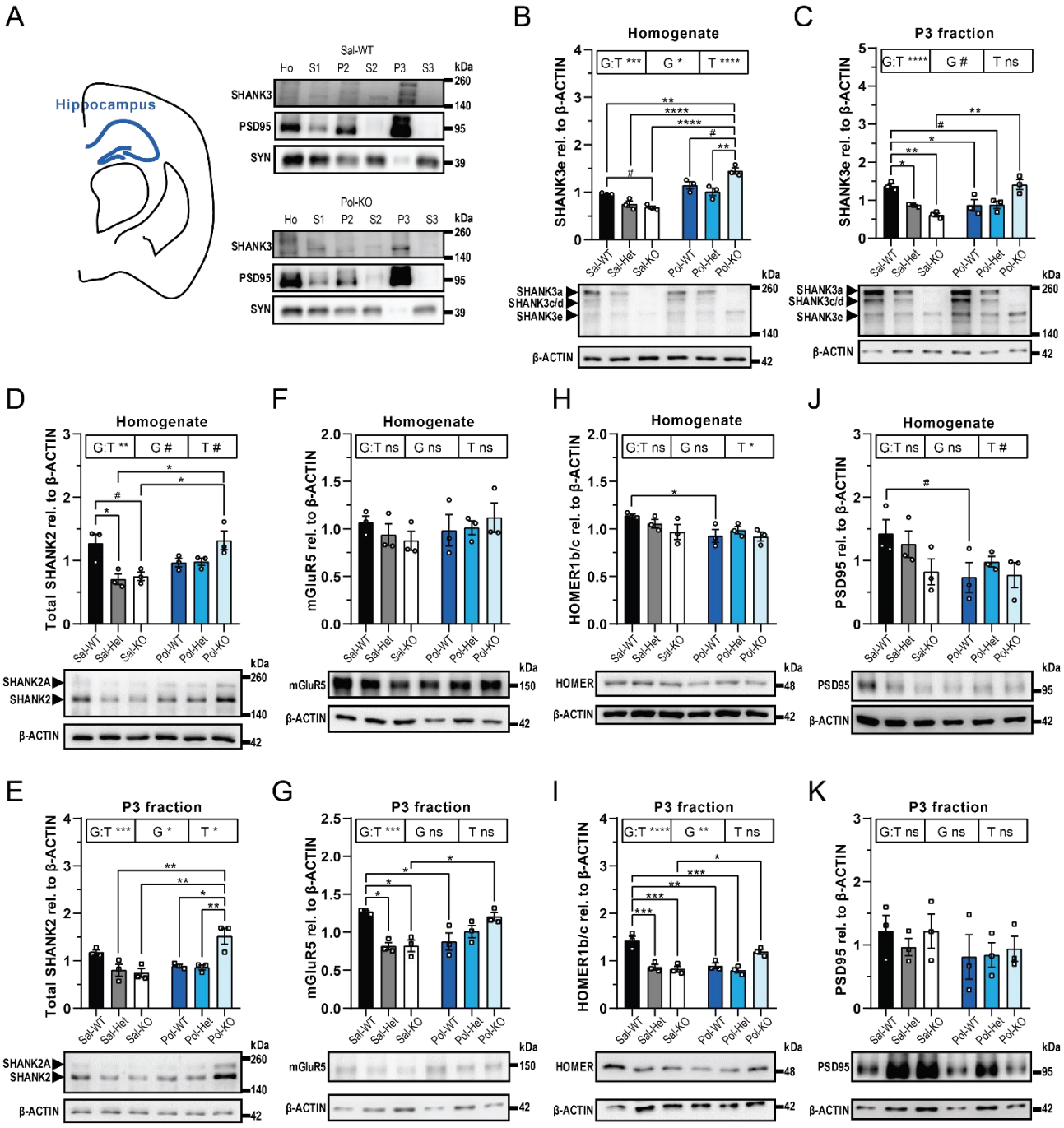

Figure 5. Synaptic changes in hippocampus of the offspring of Het dams. A Fractionation of the hippocampus. Western Blots of Sal-WT and Pol-KO are shown for SHANK3, PSD95 (postsynaptic) and SYNAPTOPHYSIN (SYN, presynaptic)**. B** Western Blot analysis for SHANK3 and β-ACTIN of hippocampus homogenate. The SHANK3e isoform was analyzed. G:T ***p=0.0007, G *p=0.0166, T ****p<0.0001, Sal-WT vs Pol-KO **p=0.0017, Sal-Het vs Pol-KO ****p<0.0001, Sal-KO vs Pol-KO ****p<0.0001, Pol-WT vs Pol-KO #p=0.0591, Pol-Het vs Pol-KO **p=0.0038, Sal-WT vs Sal-KO #p=0.0897. **C** Western Blot analysis for SHANK3 and β-ACTIN of hippocampus P3 fraction. The SHANK3e isoform was analyzed. G:T ****p<0.0001, G #p=0.0681, Sal-WT vs Sal-Het *p=0.0429, Sal-WT vs Sal-KO **p=0.0020, Sal-WT vs Pol-WT *p=0.0484, Sal-WT vs Pol-Het #p=0.0543, Pol-KO vs Sal-KO **p=0.0013. **D** Western Blot analysis for SHANK2 and β-ACTIN of hippocampus homogenate. The total SHANK2 was analysed. G:T **p=0.0035, G #p=0.0533, T #p=0.0515, Sal-WT vs Sal-Het *p=0.0317, Sal-WT vs Sal-KO #p=0.0565, Sal-Het vs Pol-KO *p=0.0172, Sal-KO vs Pol-KO *p=0.0304. **E** Western Blot analysis for SHANK2 and β-ACTIN of hippocampus

P3 fraction. The total SHANK2 was analysed. G:T ***p=0.0006, G *p=0.0309, T *p=0.0470, Sal-Het vs Pol-KO **p=0.0042, Sal-KO vs Pol-KO **p=0.0021, Pol-WT vs Pol-KO *p=0.0123, Pol-Het vs Pol-KO **p=0.0082. **F** Western Blot analysis for mGluR5 and β-ACTIN of hippocampus homogenate. **G** Western Blot analysis for mGluR5 and β-ACTIN of hippocampus P3 fraction. G:T ***p=0.0004, Sal-WT vs Sal-Het *p=0.0117, Sal-WT vs Sal-KO *p=0.0124, Sal-WT vs Pol-WT *p=0.0333, Sal-KO vs Pol-KO *p=0.0396. **H** Western Blot analysis for HOMER1b/c and β-ACTIN of hippocampus homogenate. T *p=0.0256, Pol-WT vs Sal-WT *p=0.0439. **I** Western Blot analysis for HOMER1b/c and β-ACTIN of hippocampus P3 fraction. G:T ****p<0.0001, G **p=0.0010, Sal-WT vs Sal-Het ***p=0.0007, Sal-WT vs Sal-KO ***p=0.0004, Sal-WT vs Pol-WT **p=0.0012, Sal-WT vs Pol-Het ***p=0.0003, Sal-KO vs Pol-KO *p=0.0236. **J** Western Blot analysis for PSD95 and β-ACTIN of hippocampus homogenate. T #p=0.0581, Pol-WT vs Sal-WT #p=0.0904. **K** Western Blot analysis for PSD95 and β-ACTIN of hippocampus P3 fraction. **B-K** Data were tested for normality with the Shapiro-Wilk test followed by two-way ANOVA with a Bonferroni correction for multiple comparisons. Significance level was set to 0.05 (#<0.10, *p<0.05, **p<0.01, ***p<0.001, ****p<0.0001). Mean ± SEM, n=3. G = Genotype of the offspring; T = Treatment of the mother; G:T = interaction between the two factors; ns = not significant.

The PFC, on the other hand, was not that strongly affected (Figure S13, S14 and S10C). Again, we saw an increase of SHANK3e in Pol-KO, but only in the homogenate (Figure S14B) and not in the P3 fraction (Figure S14C). SHANK2 was increased in Pol-KO in both homogenate and P3 fraction (Figure S14D and E), comparable to striatum and hippocampus. However, all the other proteins analyzed were not changed in PFC (Figure S14F-K).

To summarize the results obtained from Western Blot analysis (Figure 6A), we compared the Sal-KO to the Sal-WT groups to visualize the findings in the *Shank3Δ11-/-* mice. The animals showed a decreased expression of most of the proteins analysed. The changes were found in homogenate but more substantially in the postsynaptic P3 fraction. Most changes were found in striatum, as reported previously, the PFC was affected the least. The Poly I:C injection itself did change the expression of postsynaptic proteins in WT animals, but solely in the hippocampus. The two-hit mice (comparing Pol-KO to Sal-KO) showed an increase of proteins that previously had been downregulated in the Sal-KO mice. Again, the striatum was affected the most and the PFC the least. Regarding the behaviour (Figure 6B), the *Shank3Δ11-/-* mice (Sal-KO) exhibited changes in ASD-like core symptoms and comorbidities while the Pol-WT group displayed a mild autistic-like phenotype and only an alteration in motor coordination. When comparing the two-hit mice to the Sal-KO, only the core symptoms are aggravated but not the comorbidities. Thus, combining our biochemical and behavioural findings, the two-hit mice show elevated protein expression but compromised behavioural performance (Figure 6C). Therefore, a genetic or an environmental impact can change the synaptic protein content and, independent of a de- or increase, result in ASD-like behaviour.

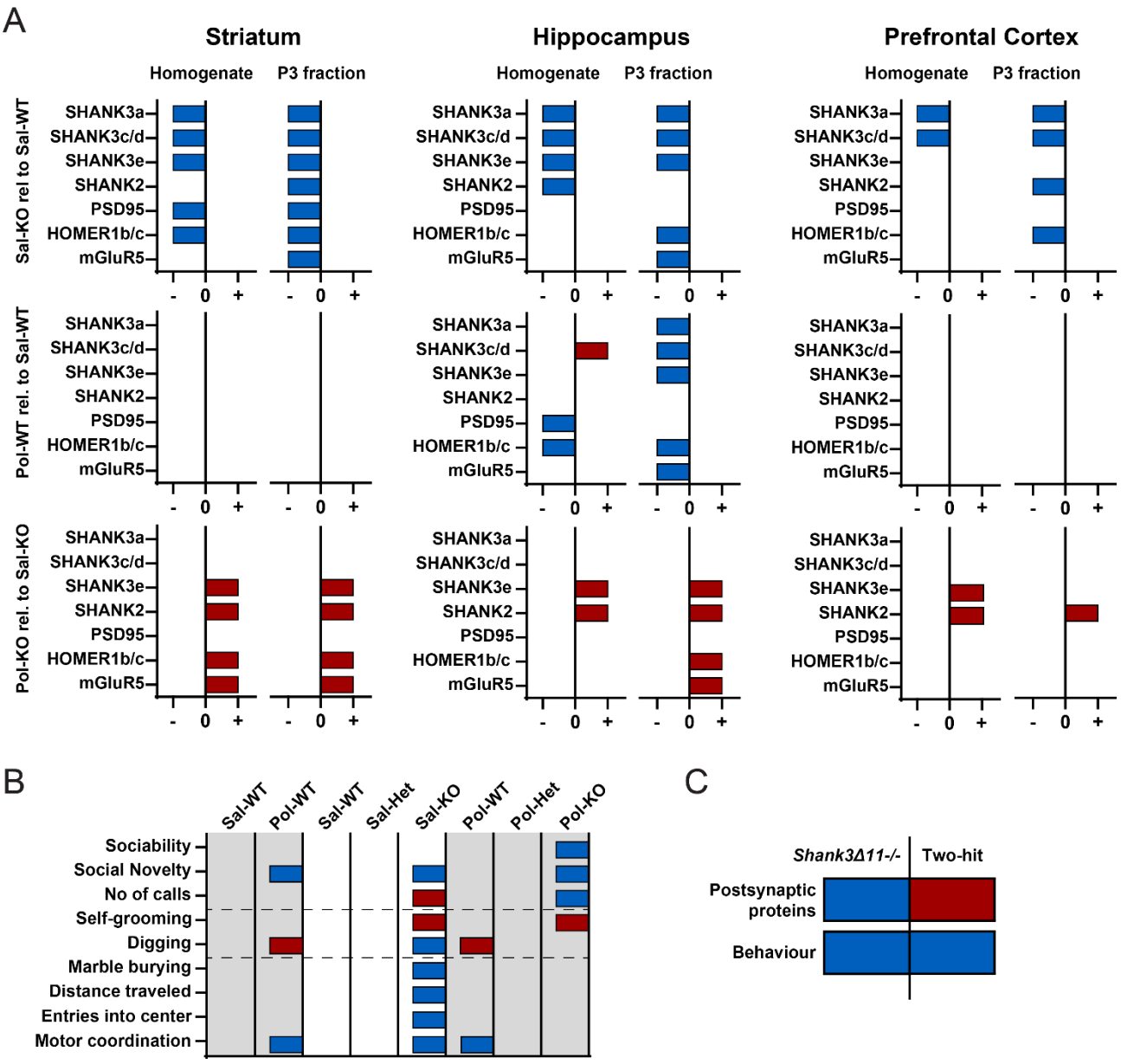

Figure 6. Summary of the results obtained in Western Blot and behaviour analysis. A General summary of all Western Blot results, indicating all the proteins affected in the Sal-KO, Pol-WT and Pol-KO groups, first in the striatum, then the hippocampus and finally in the prefrontal cortex. The effects in both the homogenate and the P3 fraction are displayed. The Sal-KO and Pol-WT groups are compared to the control (Sal-WT) whereas Pol-KO is compared to Sal-KO. **B** General summary of all behavioural results, indicating deficits in all experimental groups. All groups are compared to the control (Sal-WT) except Pol-KO which is compared to Sal-KO. The dotted lines separate the three sets of experiments, starting from the top – social behaviour, repetitive behaviour and comorbidities. No = Number. **C** Comparison between Sal-KO (*Shank3Δ11−/−*) and Pol-KO (two-hit), indicating alterations in postsynaptic proteins and behaviour. The Sal-KO group is compared to the control (Sal-WT) whereas Pol-KO is compared to Sal-KO. **A-C** A red bar indicates an increase and a blue bar indicates a decrease. The bars are not indicative of the amount of decrease or increase. Significant results ($p<0.05$) and tendencies ($p<0.10$) are displayed in the figure.

4 Conclusions

In summary, male *Shank3Δ11-/-* mice, offspring of saline-injected dams, displayed the core symptoms of autism, meaning social approach and communication deficits and increased self-grooming, together with a decrease in the expression of several postsynaptic proteins in all regions analysed, more pronounced in the PSD (postsynaptic density) than in the whole tissue lysate. Even though the immune reaction of the mother to the Poly I:C injection was severe with an increase of Interleukin 6 in the blood serum and sickness behaviour, the wild type male offspring of those dams showed only a mild autistic-like phenotype and decrease in the expression of postsynaptic proteins exclusively in the hippocampus. Finally, the maternal Poly I:C treatment seemed to have a different effect on the two-hit mice. They displayed a worsening exclusively of the core symptoms of autism while the levels of several proteins in the PSD were increased compared to the Sal-KO mice. Even though further characterization of the biochemical alterations in the two-hit mouse model is needed to understand the mechanism by which the autistic-like phenotype is exacerbated, this model seems to be a promising tool for the investigation of the interplay between genetic susceptibility and environmental factors in the context of ASD. Environmental factors are also less difficult to manipulate, meaning that treatments can more easily be developed. Future elucidation of the pathways involved in the pathophysiology of autism in this model has the potential to provide possible treatments for ASD-affected individuals.
(see additional information and supplementary figures in ***Atanasova et al., 2023***)

5 Glossary

Abbreviation / acronym	Description
ASD	Autism spectrum disorder
PMS	Phelan McDermid syndrome
Shank3Δ11-/-	Shank3 mouse model missing exon 11
Poly I:C	polyinosinic:polycytidylic acid
PSD	Postsynaptic density
USV	Ultrasonic vocalization
MIA	Maternal Immune activation

6 Bibliography

1. **Bauer HF, Delling JP, Bockmann J, Boeckers TM, Schön M Development of sex- and genotype-specific behavioral phenotypes in a Shank3 ASD mouse model for neurodevelopmental disorders. Front in Behavioural Neuroscience 9;16:1051175. doi: 10.3389/fnbeh.2022.1051175 (2023)**
2. **Atanasova E, Pérez Arévalo A, Graf I, Zhang R, Bockmann J, Lutz A, Boeckers TM Immune activation during pregnancy exacerbates ASD related alterations in Shank3-deficient mice. Mol Autism (2023) 5;14(1):1. doi: 10.1186/s13229-022-00532-3.**
3. Yildiz B, Schiedt L, Mulaw M, Bockmann J, Jesse S, Lutz A, Boeckers TM Muscular hypotonia in Shank3 related ASD is accompanied by increased intracellular Calcium concentrations and ion channel dysregulation. Front Cell Develop Biology Jul 30;5:100105. doi: 10.1016/j.crneur.2023.100105. eCollection (2023)
4. Ioannidis V, Pandey R, Bauer H, Schoen M, Bockmann J, Boeckers TM, Lutz A Disrupted extracellular matrix and cell cycle genes in autism-associated Shank3 deficiency are targeted by Lithium. Mol Psychiatry Dec 20. doi: 10.1038/s41380-023-02362-y. (2023)
5. Ahmad M, Stirmlinger N, Stifel U, Lee S, Weingandt M, Kelp U, Bockmann J, Ignatius A, Boeckers TM, Tuckermann J Downregulation of the autism spectrum disorder gene Shank2 decreases osteoblast differentiation and bone mass. JBMR plus Dec 15;7(2):e10711. doi: 10.1002/jbm4.10711. PMID: 36751416; PMCID: PMC9893268. (2023)
6. Delling JP, Bauer H, Gerlach-Arbeiter S, Schön M, Jacob Ch, Wagner J, Pedro MT, Knöll B, Boeckers TM Fingerprints of postsynaptic nanostructure are altered across brain regions in ASD-related SHANK3-deficiency. Mol Psychiatry doi: 10.1038/s41380-024-02559-9. (2024)
7. Woelfle S, Pedro M, Wagner J, Schoen M, Boeckers TM Expression profiles of the autism-related releated SHANK proteins in the human brain. BMC Biology 13;21(1):254. doi: 10.1186/s12915-023-01712-0. (2023b)

7 Annexes

Concerning the NF-kappa B mediated inflammation **UUlm** observed a problem with survival of the animals after crossing and breeding. **UUlm** therefore concentrated on the poly I:C project and continued to characterize the influence of a general inflammation on synapse morphology and molecular set up (in mice and man) and investigated inflammation signs during development in Shank3 KO brains and extended the investigations by analysing the role of Shank3 in muscle/osteoblast/neuronal development and differentiation as well as synapse morphology in mice and man.

UUlm established a double hit mouse model and combined a genetic deficiency (Shank3KO) with inflammation during pregnancy (polyI:C injection). This model was found to induce a higher abortion rate and a drop of temperature of the mother animal shortly after poly I:C injection. The basis of this study was extensive characterization of the Shank3KO mouse model and the development of autism like behaviour during development (*Bauer et al., 2023*). An extensive battery of behavioural tests and biochemical analysis have been performed to compare the double hit model with either WT-mice, the genetic model (*Shank3Δ11-/-*) alone, or the poly I:C injection alone. We show that the two-hit mice exhibit excessive grooming and deficits in social behaviour more prominently than the *Shank3Δ11-/-* mice. Interestingly these behavioural changes were accompanied by an unexpected upregulation of postsynaptic density (PSD) proteins at excitatory synapses in striatum, hippocampus and prefrontal cortex. With this study we demonstrate that there is an interplay between genetic susceptibility and environmental factors defining the severity of ASD symptoms. Moreover, we show that a general misbalance of PSD proteins at excitatory synapses are linked to ASD symptoms, making this two-hit model a promising tool for the investigation of the complex pathophysiology of neurodevelopmental disorders (*Atanasova et al. 2023*).

In close connection to the IMI/AIMS2-Trials project **UULM** furthermore focussed on structural and molecular alterations of striated muscles in PMS (*Yildiz et al., 2023*) and found increased intracellular Calcium levels and a deregulation of important ion-channels that control ion homeostasis in striated muscles cells. In an *in vitro* study, we focussed on the effect of Lithium –a potential compound to treat Shank3 related symptoms- on hippocampal neurons of WT and Shank3 KO animals (*Ioannidis et al., 2023*). We saw that Shank3 deficiency affects extracellular matrix genes as well as genes of the cell cycle. In a quite similar methodological approach we also analysed the role of Shank genes for osteoblast differentiation (*Ahmad et al., 2023*). Finally, we employed a combination of expansion microscopy and STED microscopy to analyse the substructure of excitatory synapses (*Delling et al.,*

2024). By this we were able to categorize synapses according to the complexity of the postsynaptic density (PSD). Using these categories, we identified a defined regional pattern of PSD complexity in the mouse brain. In addition, when we compared the distribution with Shank3 KO animals, we found that in all brain regions analysed the complexity is shifted to lower levels. Moreover, we optimized fluorescence stainings in archived human brain sections to closely analyse SHANK expression in the human brain (*Woelfle et al., 2023b*). In this study we especially concentrated on the expression of Shank2 and Shank3 and found that the regional expression patterns as well as expression levels are quite similar between mouse and man.